


Facile preparation of a conjugated polymer-based biosensor for glucose monitoring

Umut Bulut¹  | Şevki Can Cevher² | Vuslat Öykü Sayın¹ |
Sevgi Sarıgül Özbek¹ | Nevra Altın¹ | Ali Çırpan³ | Saniye Söylemez⁴

¹Faculty of Pharmacy, Department of Analytical Chemistry, Acıbadem Mehmet Ali Aydınlar University, Atasehir, Istanbul, Turkey

²Institute of Computational Physics, Zurich University of Applied Sciences, ZHAW, Winterthur, Switzerland

³Faculty of Science, Department of Chemistry, Middle East Technical University, Ankara, Turkey

⁴Faculty of Engineering, Department of Biomedical Engineering, Necmettin Erbakan University, Konya, Turkey

Correspondence

Umut Bulut, Faculty of Pharmacy, Department of Analytical Chemistry, Acıbadem Mehmet Ali Aydınlar University, Kayisdagi Cd. No:32, 34684 Atasehir, Istanbul, Turkey.
Email: umut.bulut@acibadem.edu.tr

Saniye Söylemez, Faculty of Engineering, Department of Biomedical Engineering, Necmettin Erbakan University, Yeni Meram Cd., Kasım Halife Sk., No: 11/1, 42090 Meram, Konya, Turkey.
Email: saniyesoylez@gmail.com

Abstract

Diabetes is an important public health problem all over the world that affects the quality of life, and its late diagnosis leads to serious complications such as stroke, blindness, limb amputations, and kidney failure. Fabrication of economical and user-friendly biosensor systems allows the rapid and early detection of prediabetes and type 2 diabetes. Accordingly, a novel, amino-functionalized, conjugated, alternating polymer was synthesized, characterized, and coated on a glassy carbon electrode (GCE) to be used as an immobilization platform for the glucose oxidase (GOx) enzyme. The decline in oxygen level due to the enzymatic reaction at a potential of -0.7 V vs. silver/silver chloride (Ag/AgCl) is screened as a biosensor response. The proposed biosensor displayed high selectivity and specificity for glucose with a broad linear range, a low detection limit, good reproducibility and repeatability, and a long shelf life. Surface modifications were characterized using cyclic voltammetry (CV) and field emission scanning electron microscopy (FE-SEM) techniques. The real-life sample application of the constructed biosensor to determine the glucose amount was performed in human serum.

KEYWORDS

amperometric glucose biosensor, conjugated polymers, enzyme immobilization, glucose oxidase

1 | INTRODUCTION

Diabetes mellitus is a chronic disease which is associated with increased risks of complications such as cardiovascular diseases, kidney failure, blindness, etc. Globally, it poses a serious threat to public health and creates an economic burden on health budgets. In 2021, approximately 537 million adults already had diabetes, which is predicted to rise to 643 million people by 2030 and 783 million people by 2045, according to the latest Diabetes

Atlas Report [1]. Regular blood glucose monitoring is crucial for the early diagnosis and effective management of diabetes, so there is a need for rapid, low cost, bedside tests. The portability and simplicity of electrochemical biosensors enable the regular monitoring of blood glucose levels at a relatively low cost compared to laboratory-based techniques such as gas chromatography-mass spectrometry (GC-MS) [2], surface plasmon resonance (SPR) [3], fluorescence [4], infrared spectroscopy [5], etc., which require qualified personnel and take

This is an open access article under the terms of the Creative Commons Attribution License, which permits use, distribution and reproduction in any medium, provided the original work is properly cited.

© 2024 The Authors. *Electroanalysis* published by Wiley-VCH GmbH.

longer analysis times. Biosensors use transducers for signal production whose amplitudes are proportional to the analyte concentration and they are widely employed in glucose detection [6].

Conjugated polymers (CPs) are useful components for the construction of biosensors due to their distinctive optoelectronic characteristics, such as biocompatibility, low detection limits, ease of production, low cost, higher sensitivity, and selectivity [7–9]. The current understanding of structure property relationships makes them great candidates for specific applications [10–12]. Donor acceptor type CPs, which is the case in this study, can provide a decreased band gap and therefore enhanced conductivity [13]. Moreover, the unique features of the monomers can be cumulatively beneficial, as benzodithiophene [14,15] cores provide fused structures with high hole transport characteristics, while amine functionalized benzene units [16–20] provide well established interaction with, in particularly binding to, biorecognition materials like enzymes, aptamers, antibodies, etc. Further, the use of CPs enhances the electrical communication between the electrode surface and the enzyme's redox center by directly wiring the enzyme to the electrode surface [21].

Amino functionalized polymers were studied previously by our group for the analyses of testosterone [20] and glucose [22] along with other groups for the detection of different analytes such as ethanol [23], organophosphorus pesticides [24], methamphetamine [25], etc. The amino functionalization of CPs is of great interest in biosensing applications due to their ability to form strong bonds between biorecognition elements and sensory platforms, giving rise to high-performance bio-detection/sensing device parameters. In a study where phenylenediamines (o-, m-, p- derivatives) were electrochemically polymerized onto a platinum electrode to investigate performance criteria for glucose sensing, it was revealed that poly-m-phenylenediamine exhibited superior sensitivity and lower permeability to interfering substances like ascorbic acid and L-dopamine [26]. In another study, a biosensor constructed by electropolymerization of 2,6-diaminopyridine on a GCE modified with multi-walled carbon nanotubes showed a high performance with a broad linear range between 0.42 μ M and 8.0 mM, and a considerably good repeatability (1.6%) [27].

Two dimensional conjugation in organic electronic materials is obtained by introducing or infusing a secondary aromatic ring/structure into the conjugated polymer backbone. High performance devices were obtained by enhancing morphology and effectively increasing the charge carrier properties of the device [28]. Moreover, effective and fine tuning the highest occupied molecular

orbital and lowest unoccupied molecular orbital levels, absorption and/or emission profiles, and thermogravimetric features are of great interest in two dimensional architectural design foresight [29].

The choice of an appropriate matrix and the immobilization procedure are the most critical factors in the fabrication of biosensors. Herein, we report the construction of a highly sensitive glucose biosensor in which GOx is immobilized on the poly(benzenediamine-bis[(2-ethylhexyl)oxy]benzodithiophene) platform [P(BD TT-BDA)] for the first time. We investigated the role of the polymeric surface composed of benzodithiophene and benzenediamine moieties on the characteristics of the biosensor to provide a convenient surface for optimized enzyme immobilization. The conjugated polymer, thus, possesses powerful features for biosensor applications, such as easy and direct deposition on the electrode surface, redox conductivity, rapid response, and enhanced stability of the biosensor. An alkyl thienyl group to the benzodithiophene moiety was introduced for increased charge transport properties and coupled with the benzenediamine moiety to make a strong interaction between the electrode and the sensory biorecognition element "GOx". Moreover, strong π - π stacking between aromatic moieties in the polymer and aromatic residues of the enzyme enables a sensitive and reliable biosensor by conserving the structure of biological molecules during the enzymatic reaction. In summary, the aim here is twofold: introducing a novel substance to the literature and developing a new sensor platform that will serve as a model for existing studies via achieving by one-step immobilization of GOx onto the conjugated polymer. The concentrations of the polymer, enzyme, and crosslinker are optimized along with the pH value. FE-SEM and CV are employed to examine changes to the electrode surface. Amperometry was used to measure the amount of glucose by measuring the decrease in oxygen concentration in the medium due to enzyme activity. Analytical characteristics are investigated for changes due to surface modifications and interactions with glucose. The glucose content in an artificial human serum sample was determined to verify the biosensor's accuracy.

2 | EXPERIMENTAL

2.1 | Chemicals

1,1'-[4,8-Bis[5-(2-ethylhexyl)-2-thienyl]benzo[1,2-*b*:4,5-*b'*]dithiophene-2,6-diyl]bis[1,1,1-trimethylstannane] (BD TT) and other chemicals used in the synthesis were obtained from Sigma Aldrich (St. Louis, MO, USA). HPLC grade tetrahydrofuran (THF) was bought from

Sigma Aldrich, and it was distilled under nitrogen atmosphere in the presence of benzophenone/sodium (from a local company) prior to use. 3,6-dibromobenzene-1,2-diamine (BDA) was synthesized previously as described [30]. The Stille polymerization reaction was carried out under N_2 atmosphere. Glutaraldehyde (GA, Grade II, 25% in H_2O), GOx (beta-D-glucose: oxygen 1-oxidoreductase, EC 1.1.3.4, $\geq 100,000$ units/g solid from *A. niger*), potassium ferricyanide(III) ($K_3Fe(CN)_6$), potassium hexacyanoferrate(II) trihydrate ($K_4Fe(CN)_6 \cdot 3H_2O$) and artificial human serum samples (H4522-Human male AB plasma-sterile filtered) were purchased from Sigma Aldrich. Potassium chloride (KCl), sodium acetate anhydrous (CH_3COONa), and sodium phosphate dibasic (Na_2HPO_4) were obtained from AFG Bioscience (AFG Bioscience, Wood Dale, IL, USA). D-glucose anhydrous was purchased from BioFroxx (Einhausen, Germany). All chemicals were used as received. Sodium phosphate dibasic (Na_2HPO_4) and sodium acetate anhydrous (CH_3COONa) were utilized in preparing the buffer solutions.

2.2 | Instrumentations

Bruker Spectrospin Avance DPX-400 Spectrometer (400 MHz, Billerica, MA) was employed for Nuclear Magnetic Resonance (NMR) spectrum where tetramethylsilane (TMS) was used as an internal standard. Gel permeation chromatography (GPC) was carried out using Shimadzu RID-20 A (Kyoto, Japan) to determine weight average molecular weight (M_w) and number average molecular weight (M_n), which was calibrated against polystyrene standards operated with Polymer Standard Service styrene-divinylbenzene (PSS SDV) analytical linear column and chloroform was used as mobile phase at oven temperature of $40^\circ C$. All electrochemical measurements were performed with a Gamry 600+ potentiostat (Gamry Instruments, Warminster, PA). GCE (rod, 3 mm diameter, 0.07 cm^2 area), platinum wire, and Ag/AgCl electrodes were used as working, auxiliary, and reference electrodes, respectively. Surface characterizations were conducted with Field Emission Scanning Electron

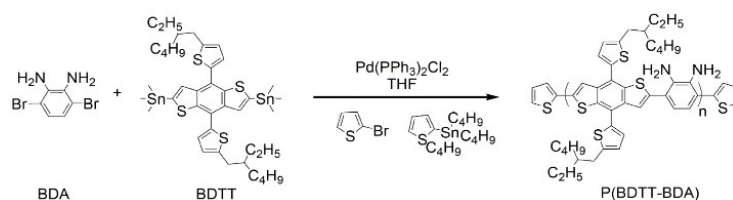
Microscopy (Zeiss GeminiSEM 500, Jena, Germany). The experiments were carried out at room temperature ($25^\circ C$), and the results show the average of three measurements taken under identical conditions. The results were given as $\pm SD$ show the average of three measurements taken under identical conditions.

2.3 | Synthesis of the alternating copolymer

BDA (91.7 mg, 0.345 mmol, 1 eq) and BDTT (312 mg, 0.345 mmol, 1 eq) were dissolved in dry THF and bubbled by N_2 for 15 min. After adding bis(triphenylphosphine)palladium(II)dichloride catalyst, the reaction mixture was refluxed for three days (Scheme 1). Tributyl(thiophen-2-yl)stannane (257 mg 0.690 mmol, 2 eq) was added and reacted for 6 h, followed by the addition of 2-bromothiophene (225 mg 1.38 mmol, 4 eq) as end cappers, which was allowed to react for 12 h. The solution was allowed to cool and was concentrated under reduced pressure. The resulting polymer was then precipitated in methanol. The solid was filtered and subjected to Soxhlet extraction with methanol, hexane, and THF, respectively. 50 mg of quadrasil (3-mercaptopropyl-functionalized silica gel) was added to the recovered polymer in THF and stirred for an hour using a magnetic stirrer. After filtering the quadrasil through laboratory filter paper, THF was removed under reduced pressure. The concentrated polymer solution was then poured into methanol, resulting in a brown solid polymer (165 mg, yield 70%). GPC: $M_n = 2.8\text{ kDa}$ $M_w = 4.2\text{ kDa}$, PDI (polydispersity index) = 1.5. 1H NMR (in $CDCl_3$) spectrum displayed broad bands in aliphatic and aromatic regions following the general trends of CPs.

2.4 | Preparation of the GOx biosensor

Biosensors were prepared after polishing the surfaces of the GCEs by using $3\text{ }\mu\text{m}$ diamond and $1\text{ }\mu\text{m}$ alumina slurry. P(BD TT-BDA) solution was prepared by dissolving 0.30 mg of P(BD TT-BDA) in $400.0\text{ }\mu\text{L}$ chloroform ($CHCl_3$) and the working electrode (WE) was coated by

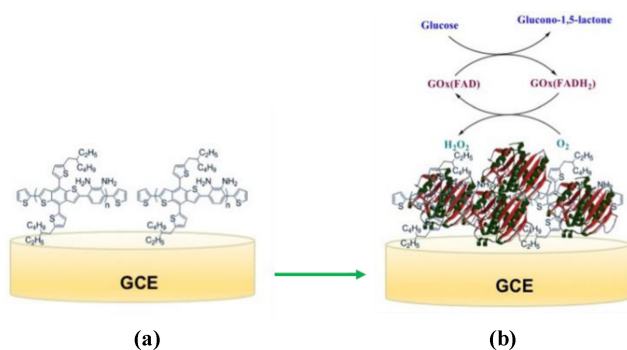


S C H E M E 1 Synthesis of P(BD TT-BDA).

adding 10.0 μL of this solution. After evaporation of CHCl_3 at room temperature, 2.50 μL of GOx prepared by dissolving 1.00 mg in 25 μL buffer solution and 5.00 μL of GA solutions were dropped, respectively, to the surface of GCE, which has already been modified by P-(BDTT-BDA) solution. The electrode was allowed to dry for 1.5 h, then rinsed with distilled water to eliminate any potential impurities from the surface. The biosensor construction is summarized in Scheme 2.

2.5 | Electrochemical measurements

A three-electrode electrochemical cell was set up by using Ag/AgCl as the reference, platinum wire as the counter and the modified GCE as the working electrode. Amperometry was used to record the biosensor measurements at -0.7 V vs. an Ag/AgCl electrode. All chronoamperometric measurements were performed in 10.0 mL of buffer solution (pH = 5.5) under a constant potential (-0.7 V) vs. Ag/AgCl electrode at room temperature. CV analysis was conducted in a solution containing 8.9 mL of acetate buffer solution having a pH of 5.5, 1.0 mL of 1.0 M KCl, 50.0 μL of 0.5 mM $\text{Fe}(\text{CN})_6^{3-}$ and 50.0 μL of 0.5 mM $\text{Fe}(\text{CN})_6^{4-}$. The potential range was from -0.4 to 0.6 V and the scan rate was 100 mV/s. After each measurement, the electrochemical cell and the electrodes were rinsed with distilled water. Before and after glucose addition, equilibrium in current was established and the difference in current between two equilibrium states was determined as the response of the fabricated biosensor. This change results from the decrease in the amount of oxygen, which is due to the reaction between GOx and glucose in the electrochemical cell. In real sample applications, the serum samples were used as received.



Scheme 2 Basic presentation of the biosensor construction: (a) P(BD TT-BDA) coated GCE, (b) GOx immobilized electrode surface.

3 | RESULTS AND DISCUSSION

3.1 | Optimization studies

The fabricated biosensor must be optimized in order to obtain reproducible measurements and better performance. In this work, the amount of P(BD TT-BDA), GOx, GA, and pH of the buffer solution were optimized, respectively, at room temperature. In each experiment, only one parameter has been changed while the others have been kept constant. In all optimization studies, 0.75 mM glucose solution was used in order to see the change in current. Firstly, the polymer concentration was optimized by analyzing solutions with different amounts of P(BD TT-BDA) in the range of 0.25–1.25 mg in CHCl_3 . In this step, the electrode surfaces were modified with polymer solutions separately, then 1.00 mg of GOx prepared by dissolving in 25 μL buffer solution having pH of 7.0 and 5.00 μL of 1% GA solutions (prepared by diluting with phosphate buffer solution having pH 7.0) were immobilized on the polymer modified surfaces and the measurements were taken in the buffer solution having a pH of 7.00 in the optimization experiments. Low responses were obtained with both high and low amounts of polymer in comparison to 0.75 mg/mL polymer containing GCE surface due to the unfavorable redox performance between the electrode surface and the active side of the enzymes caused by extremely thick or thin polymer coatings. The highest change in current after the addition of glucose was obtained with the biosensor coated with a 0.75 mg/mL polymer solution, as seen in Figure 1a. Therefore, a polymer solution with this concentration is employed for coating the surface of WE's for further experiments. Secondly, different amounts of GOx (0.25, 0.50, 0.75, and 1.00 mg) were immobilized into the surface of GCE in order to see its effect on the signal change in current with the addition of glucose. During these optimization studies, the concentration of polymer and the GA solutions were 0.75 mg polymer in 1.0 mL CHCl_3 and 1%, respectively. According to the recorded measurements given in Figure 1b, the highest signal was determined with the GCE containing 0.75 mg of enzyme. The lower amounts of enzyme (0.25 and 0.50 mg) may not be sufficient for proper enzyme immobilization. On the other hand, at high enzyme concentrations, the active site of the enzyme cannot interact properly with glucose due to steric hindrance, leading to a lower response.

After optimum values were found for the polymer and the enzyme, the concentration of GA was optimized. GA solutions were prepared as 0.50, 0.75, 1.00, 1.25, and 1.50% by diluting the commercially available GA stock solution with the buffer solution having a pH of 7.0 in

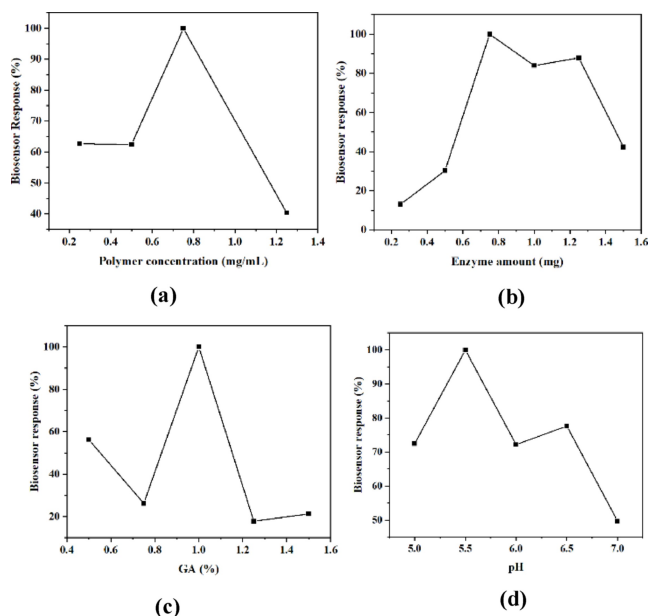


FIGURE 1 The effect of changes in a) the amount of polymer; b) the amount of GOx; c) GA concentration; and d) pH of buffer solution on the signal change in current after the addition of 0.75 mM glucose solution.

the modification of the biosensor surface, which was already coated with the polymer and the GOx solutions. Lower biosensor responses in the cases of lower GA concentrations can be attributed to insufficient immobilization of the enzyme. At higher GA concentrations, excessive binding of the enzyme molecule on the surface of the P(BDIT-BDA) matrix may lead to the loss of its proper conformation, leading to a low biosensor response. Therefore, the optimum concentration of GA was determined to be 1.00% (in buffer) for the best current signal in the presence of glucose.

Furthermore, it was shown that the biosensor response depends on the pH of the buffer solution used in electrochemical measurements [31]. Therefore, buffer solutions having different pH in the range of 5.00–8.00, in which catalytic activity of GOx is observed, were tested in order to obtain the optimum pH value. The graph drawn for the signal change vs. pH of the buffer solution (Figure 1d) shows that the maximum change in current is obtained in the buffer solution with a pH of 5.50. The charges on the enzyme's active site, depending on the pH of the medium, may affect the conformation of the enzyme's active site and hence change the activity of the enzyme. As pH increased to 5.5 from 5.0, the biosensor response increased as well. However, further increases in pH (6.0, 6.5 and 7.0) led to a decrease in the signal that might cause enzyme denaturation. This might be due to the change in the conformation of the active site

in the enzyme being less favorable for the reaction with glucose.

3.2 | Analytical characterization

A calibration curve was drawn for the response of the biosensor fabricated under optimized conditions to the addition of different amounts of glucose (Figure 2). The linear range was determined between 0.1 and 1.0 mM glucose concentration with the equation $y = 2.09x - 0.0828$ having an R^2 value of 0.996 and the sensor sensitivity was computed as $29.86 \mu\text{A}/\text{mM cm}^2$. The limit of detection (LOD) and the limit of quantification (LOQ) were determined as 0.0172 mM and 0.0521 mM, respectively. The LOD and LOQ values were determined using the following equations: $\text{LOD} = 3.3 s/m$ and $\text{LOQ} = 10 s/m$. Here, 's' represents the standard deviation, while 'm' is the slope of the calibration curve.

The Michaelis–Menten constant (K_M^{app}) and the maximum current (I_{max}) were calculated as 2.023 mM and $6.618 \mu\text{A}$ from the Lineweaver–Burk graph [32]. K_M^{app} shows the affinity of the enzyme to the substrate and a low value suggests that the enzyme has a high affinity for the substrate [33].

Numerous examples of electrochemical sensors based on CPs have been described in the literature for glucose detection. Gokoglan et al. coated paper-based electrodes with graphene and altered them further via a conducting polymer end capped with a 2,5-diphenyl-1,2,4-oxadiazole

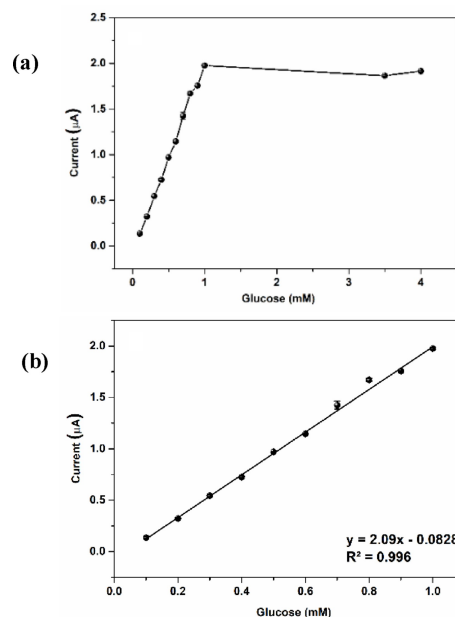


FIGURE 2 The calibration graphs for the response of the fabricated biosensor with respect to the concentration of glucose: (a) whole range, (b) linear range.

end cap, which then provided a platform for the physical adsorption of GOx using gold nanoparticles (AuNPs) [34]. A chronoamperometric glucose biosensor was devised by electrodeposition of a nanocomposite film composed of electropolymerized poly(3-aminobenzoic acid) and platinum/reduced graphene oxide on a screen-printed carbon electrode. GOx was then immobilized on the modified electrode surface using N-ethyl-N'-(3-(dimethylamino)propyl)carbodiimide/N-hydroxysuccinimide chemistry [35]. Jiménez-Fiérrez et al. developed an amperometric glucose biosensor by electropolymerization of poly(Azure A) on activated screen-printed carbon electrodes and electrodeposition of platinum nanoparticles (PtNPs) where GOx was immobilized [36]. Another GOx-based electrochemical sensor was constructed using poly(3,4-ethylenedioxythiophene):poly(styrene sulfonate) CP and electrospun-nanofibrous-membrane silicon carbide nanoparticles on chromium and gold coated glass electrodes [37]. Similarly, an enzymatic sensing platform was prepared with functionalized multi-walled carbon nanotubes and an electrospun poly(3-aminobenzylamine) fiber film [38]. Moreover, Niamsi et al. developed a paper-based biosensor on a screen-printed ionic liquid/graphene electrode modified with MXene ($\text{Ti}_3\text{C}_2\text{T}_x$), prussian blue (PB), and GOx and further coated with Nafion to prevent interference effect [39]. In addition, Li et al. fabricated a glucose sensor using GOx immobilized hydroxy fullerene/multi-walled carbon nanotubes and further modifying with Nafion [40]. These reported biosensors displayed satisfactory analytical performances, however, required several modification steps for their fabrication, whereas only a polymer layer was utilized in this work for enzyme immobilization without compromising the sensor performance. The success of the proposed sensor relies on properly immobilizing GOx on

the polymer-coated surface to prevent any leakage. This is achieved by using GA as a spacer, which reduces steric hindrance between the enzyme and the support. P-(BDTT-BDA)/GOx sensor has a broad linear range and can detect glucose at lower concentrations compared to most of the given examples. Compared to the several studies in literature, it has high sensitivity and the K_M^{app} of the proposed sensor displays a higher affinity to glucose. Table 1 features a comparison of the analytical parameters of the proposed sensing platform with previous examples in the literature.

The proposed biosensor was examined in terms of repeatability by recording its amperometric responses in the presence of 0.4 mM glucose in the reaction medium five times successively on the same electrode. The RSD% of these measurements was calculated as 5.47%, demonstrating good repeatability. For testing the reproducibility, the change in current of two separate sensors to the addition of 0.60 mM glucose at the optimized conditions was measured and the relative standard deviation (%RSD) value was computed as 1.52%, indicating good reproducibility.

Biosensor selectivity was studied using several interfering substances, including citric acid, urea, ascorbic acid, and paracetamol. The signal change was investigated for the addition of first glucose and then interfering chemical solutions, as well as for the addition of interfering chemicals first and then glucose. In these experiments, 20.0 μL 0.25 M of citric acid, urea and ascorbic acid and also 50.0 μL 0.10 M of paracetamol were used as interference. The results demonstrated that the produced biosensor gave a signal only for the addition of 40.0 μL of 0.10 M glucose but not for the other molecules (Figure 3a), leading to the conclusion that it is solely specific to glucose.

TABLE 1 Analytical features of conjugated polymer-based electrochemical glucose biosensors.

Modified electrode	Linear range [mM]	LOD [μM]	Sensitivity [$\mu\text{A}/(\text{mM cm}^2)$]	K_M^{app} [mM]	Ref.
PFLO/AuNPs/graphene/GOx	0.10–1.5	81.0	7.36	0.229	[34]
Pt/rGO/P3ABA/GOx	0.25–6.0	44.3	22.01	3.54	[35]
aSPCEs/PAA/PtNPs/GOx	0.020–2.30	7.60	42.70	14.5	[36]
Au/SiCNPs-PEDOT:PSS-PVDF-ENFM/GOx	0.50–20	0.56	30.75	NR	[37]
PABA/f-CNTs/GOx	0.56–2.8	67.0	40.00	NR	[38]
PB/ $\text{Ti}_3\text{C}_2\text{T}_x$ /GOx/Nafion/SPIL-GE	0.080–15	24.5	NR	NR	[39]
NF-GLA/MWCNTs-BSA-HFs-GOx/GCE	0.010–3.5	17.0	20.31	0.660	[40]
P(BD TT-BDA)/GOx	0.10–1.0	17.2	29.86	2.02	This work

Abbreviations: aSPCEs, activated screen-printed carbon electrodes; BSA, bovine serum albumin; ENFM, electrospun-nanofibrous-membrane; HFs, hydroxy fullerene; MWCNTs, multi-walled carbon nanotubes; NF-GLA, nafion-glutaraldehyde; NR, not reported; P3ABA, poly(3-aminobenzoic acid); PAA, poly(Azure A); PABA/f-CNTs, poly(3-aminobenzylamine) functionalized multi-walled carbon nanotubes; PB, prussian blue; P(BD TT), poly(benzenediamine-bis[(2-ethylhexyl)oxy]benzodithiophene); PEDOT, poly(3,4-ethylenedioxythiophene); PSS, poly(styrene sulfonate); Pt, platinum; PVDF, polyvinylidene fluoride; rGO, reduced graphene oxide; SiCNP, silicon carbide nanoparticles; SPIL-GE, screen-printed ionic liquid/graphene electrode.

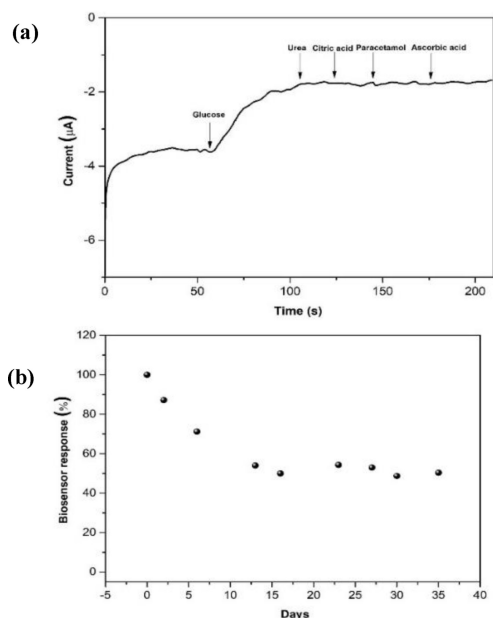


FIGURE 3 (a) Amperometric responses of P(BD TT-BDA) to glucose and interfering compounds. (b) Biosensor shelf life.

The storage time of the biosensor was investigated during a 35-day period by the addition of 0.50 mM glucose solution into the electrochemical measurement cell, which already had 10 mL of buffer solution at pH 5.5 and their amperometric responses are shown in Figure 3b. According to the results, after 35 days, the biosensor retained 50% of its initial response. When not in use, it was kept in storage at 4 °C. The immobilization matrix and enzyme molecules are covalently linked, which relatively increases the shelf life.

3.3 | Surface characterization

Effective surface areas of electrodes were calculated according to the Randles–Sevcik equation to follow how changing the electrode impacts the behavior of the redox couple in the solution [41]. Bare, P(BD TT-BDA), and P(BD TT-BDA)/GOx modified GCEs were prepared for this purpose and their current responses were compared. According to the current responses, the effective surface areas were estimated as 5.00, 0.14, and 0.097 mm², respectively. As seen in Figure 4, the P(BD TT-BDA) modified electrode showed a higher current response than the other one. As the biomolecule is an insulator, there is a decrease in oxidation current after GOx modification on the polymer surface. Even though the conductivity values decreased compared to the bare electrode with the additional layers on the electrode surfaces, the electrode surfaces were sufficient for efficient electron transfer.

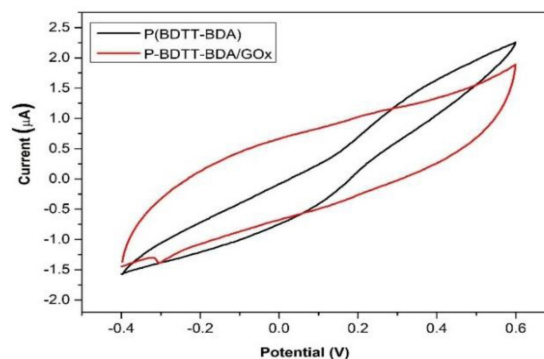


FIGURE 4 Cyclic voltammograms of P(BD TT-BDA) and P(BD TT-BDA)/GOx in 5 mM Fe(CN)₆^{3-/4-} 0.1 M KCl, pH 5.5 buffer solution.

Figure 5 shows SEM images of P(BD TT-BDA) (A) and P(BD TT-BDA)/GOx. The P(BD TT-BDA)-coated surface had a smooth surface, whereas the other had a homogeneous porous surface. This means that after enzyme immobilization, enzyme molecules completely cover all of the P(BD TT-BDA) surfaces.

3.4 | Real sample analysis

The detection of glucose with the proposed biosensor was tested in real samples to demonstrate the applicability of the proposed biosensor. For this reason, the serum samples were fortified with glucose and certain amounts were injected into the reaction medium. The biosensor responses and theoretical values were compared with each other and summarized in Table 2. The fabricated biosensor gave no amperometric response to the addition of the unspiked samples. However, after the serum samples were spiked with glucose, the biosensor gave a response and the results are summarized in Table 2. These results show that the P(BD TT-BDA)/GOx biosensor can be used effectively for the detection of glucose in real samples.

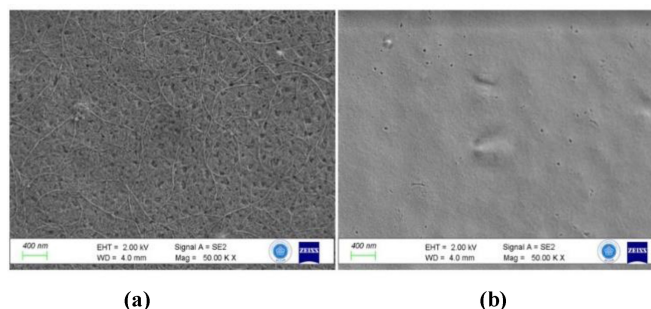


FIGURE 5 SEM images of (a) P(BD TT-BDA); (b) P(BD TT-BDA)/GOx at optimum conditions.

TABLE 2 Determination of glucose in human serum samples.

Spiked with glucose (mmol/L)	Found with biosensor (mmol/L)	Recovery (%)
0.30	0.304 ± 0.0055	101.59
0.50	0.502 ± 0.0034	100.37

4 | CONCLUSIONS

In this work, an efficient, highly sensitive, and practical amperometric glucose biosensor was developed. The fabrication of the sensor involved the one-step immobilization of GOx onto the conjugated polymer with benzodithiophene and benzenediamine moieties through covalent bonding with amino groups. The biosensor displayed excellent analytical performance with a wide linear range and low LOD, possessing repeatability and long-term stability. High selectivity towards glucose was shown as no interference effect was detected. An artificial serum sample spiked with glucose was tested to demonstrate the utilization of the designed biosensor on real samples. The P(BDTP-BDA)-modified biosensor mostly exhibits improved characteristics for glucose sensing compared to previous studies reported in the literature. Moreover, it provides versatility and a viable method to fabricate other biosensors using alternative enzymes, such as alcohol oxidase and tyrosinase, enabling the real-time detection of various analytes in clinical applications.

CONFLICT OF INTEREST STATEMENT

The authors declare no conflict of interest.

DATA AVAILABILITY STATEMENT

The data that support the findings of this study are available from the corresponding author upon reasonable request.

ORCID

Umut Bulut  <http://orcid.org/0000-0002-4282-5233>

REFERENCES

- International Diabetes Federation, IDF Diabetes Atlas, **2021**, <https://www.diabetesatlas.org>.
- P. N. Wahjudi, M. E. Patterson, S. Lim, J. K. Yee, C. S. Mao, W. N. P. Lee, *Clin. Biochem.* **2010**, *43*, 198–207.
- D. Li, J. Su, J. Yang, S. Yu, J. Zhang, K. Xu, H. Yu, *Biomed. Opt. Express* **2017**, *8*, 5206–5217.
- J. C. Pickup, F. Hussain, N. D. Evans, O. J. Rolinski, D. J. Birch, *Biosens. Bioelectron.* **2005**, *20*, 2555–2565.
- W. Villena Gonzales, A. T. Mobashsher, A. Abbosh, *Sensors* **2019**, *19*, 800.
- Z. Peng, X. Xie, Q. Tan, H. Kang, J. Cui, X. Zhang, W. Li, G. Feng, *J. Innov. Opt. Health Sci.* **2022**, *15*, 2230003.
- B. D. Malhotra, A. Chaubey, S. P. Singh, *Anal. Chim. Acta* **2006**, *578*, 59–74.
- K. Arshak, V. Velusamy, O. Korostynska, K. Oliwa-Stasiak, C. Adley, *IEEE Sens. J.* **2009**, *9*, 1942–1951.
- T. H. Le, Y. Kim, H. Yoon, *Polymers* **2017**, *9*, 150.
- T. Lei, J.-Y. Wang, J. Pei, *Acc. Chem. Res.* **2014**, *47*, 1117–1126.
- L. Jiang, J. D. Hirst, H. Do, *J. Phys. Chem. C* **2022**, *126*, 10842–10854.
- X. Chi, Q. Chen, Z. Lan, X. Zhang, X. Chen, X. Wang, *Chem. – A Eur. J.* **2023**, *29*, e202202734.
- M. C. Scharber, N. S. Sariciftci, *Adv. Mater. Technol.* **2021**, *6*, 202000857.
- E. A. Gaml, A. Dubey, K. M. Reza, M. N. Hasan, N. Adhikari, H. Elbohy, B. Bahrami, H. Zeyada, S. Yang, Q. Qiao, *Sol. Energy. Mater. Sol. Cells* **2017**, *168*, 8–13.
- R. Sandoval-Torrientes, I. Zimmermann, J. Calbo, J. Aragón, J. Santos, E. Ortí, N. Martín, M. K. Nazeeruddin, *J. Mater. Chem. A* **2018**, *6*, 5944–5951.
- T. Yao, K. Takashima, *Biosens. Bioelectron.* **1998**, *13*, 67–73.
- A. Curulli, F. Valentini, S. Orlanduci, M. L. Terranova, G. Palleschi, *Biosens. Bioelectron.* **2004**, *20*, 1223–1232.
- E. Akyilmaz, O. Kozgus, H. Türkmen, B. Çetinkaya, *Bioelectrochemistry* **2010**, *78*, 135–140.
- G. E. Fenoy, W. A. Marmisollé, O. Azzaroni, W. Knoll, *Biosens. Bioelectron.* **2020**, *148*, 111796.
- U. Bulut, S. Sanli, S. C. Cevher, A. Cirpan, S. Donmez, S. Timur, *J. Appl. Polym. Sci.* **2020**, *137*, 49332.
- J. Wang, *Chem. Rev.* **2008**, *108*, 814–825.
- U. Bulut, V. O. Sayin, S. C. Cevher, A. Cirpan, S. Soylemez, *Express Polym. Lett.* **2022**, *16*, 1012–1021.
- N. C. Kecec, F. E. Kanik, Y. Arslan Udum, C. G. Hizliates, Y. Ergun, L. Toppare, *Sens. Actuators B Chem.* **2014**, *193*, 306–314.
- M. Kesik, F. E. Kanik, J. Turan, M. Kolb, S. Timur, M. Bahadir, L. Toppare, *Sens. Actuators B Chem.* **2014**, *205*, 39–49.
- B. Demir, T. Yilmaz, E. Guler, Z. P. Gumus, H. Akbulut, E. Aldemir, H. Coskunol, D. G. Colak, I. Cianga, S. Yamada, S. Timur, *Talanta* **2016**, *161*, 789–796.
- D. M. Zhou, Y. Q. Dai, K. K. Shiu, *J. Appl. Electrochem.* **2010**, *40*, 1997–2003.
- M. A. Kamyabi, N. Hajari, A. P. Turner, A. Tiwari, *Talanta* **2013**, *116*, 801–808.
- C. Cui, Z. He, Y. Wu, X. Cheng, H. Wu, Y. Li, Y. Cao, W. Y. Wong, *Energy Environ. Sci.* **2016**, *9*, 885–891.
- L. Ye, S. Zhang, L. Huo, M. Zhang, J. Hou, *Acc. Chem. Res.* **2014**, *47*, 1595–1603.
- A. Tanimoto, T. Yamamoto, *Adv. Synth. Catal.* **2004**, *46*, 1818–1823.
- H. J. Brights, M. Appleby, *J. Biol. Chem.* **1969**, *244*, 3625–3634.
- H. Lineweaver, D. Burk, *J. Am. Chem. Soc.* **1934**, *56*, 658–666.
- C. Chen, Y. Jiang, J. Kan, *Biosens. Bioelectron.* **2006**, *22*, 639–643.

34. T. C. Gokoglan, M. Kesik, S. Soylemez, R. Yuksel, H. E. Unalan, L. Toppare, *J. Electrochem. Soc.* **2017**, *164*, G59–G64.
35. S. Phetsang, J. Jakmunee, P. Mungkornasawakul, R. Laocharoensuk, K. Ounnunkad, *Bioelectrochemistry* **2019**, *127*, 125–135.
36. F. Jiménez-Fiérrez, M. I. González-Sánchez, R. Jiménez-Pérez, J. Iniesta, J. E. Valero, *Sensors* **2020**, *20*, 4489.
37. K. Puttananjegowda, A. Takshi, S. Thomas, *Biosens. Bioelectron.* **2021**, *186*, 113285–113289.
38. S. Sriwichai, S. Phanichphant, *Express Polym. Lett.* **2022**, *16*, 439–450.
39. W. Niamsi, N. Larpant, P. K. Kalambate, V. Primpray, C. Karuwan, N. Rodthongkum, W. Laiwattanapaisal, *Biosensors* **2022**, *8*, 852.
40. Y.-Y. Li, X.-X. Ma, X.-Y. Song, L.-L. Ma, Y.-Y. Li, X. Meng, Y.-J. Chen, K.-X. Xu, A. A. Moosavi-Movahedi, B.-L. Xiao, J. Hong, *Sensors* **2023**, *23*, 3209.
41. A. J. Bard, L. R. Faulkner, in *Electrochemical Methods: Fundamentals and Applications*, 2nd ed., Wiley, New York **2001**, pp. 228–230.

How to cite this article: U. Bulut, Ş. C. Cevher, V. Ö. Sayın, S. S. Özbek, N. Altın, A. Çırpan, S. Söylemez, *Electroanalysis* **2024**, *36*, e202300365.
<https://doi.org/10.1002/elan.202300365>

Graphical Abstract

The contents of this page will be used as part of the graphical abstract of html only.
It will not be published as part of main.

